

Contents lists available at ScienceDirect

Urban Climate

journal homepage: <http://www.elsevier.com/locate/uclim>



GIS-based mapping of Local Climate Zone in the high-density city of Hong Kong



Yingsheng Zheng^{a,*}, Chao Ren^{a,b,c}, Yong Xu^c, Ran Wang^a, Justin Ho^b, Kevin Lau^c, Edward Ng^{a,b,c}

^a School of Architecture, The Chinese University of Hong Kong, Hong Kong

^b Institute of Environment, Energy and Sustainability, The Chinese University of Hong Kong, Hong Kong

^c Institute of Future Cities, The Chinese University of Hong Kong, Hong Kong

ARTICLE INFO

Article history:

Received 14 October 2016

Received in revised form 17 May 2017

Accepted 21 May 2017

Keywords:

Local Climate Zone

High-density city

Raster-based GIS method

Sensitivity test

Urban morphology analysis

ABSTRACT

This study aims to develop a Local Climate Zone (LCZ) classification map and establish the associated urban morphology database as a cross-discipline information platform for climate research and planning decision making in Hong Kong. Geographic information system (GIS) was applied to synergize various kinds of planning data, and classify land surface properties following the LCZ framework.

Sensitivity tests were performed to identify the appropriate raster resolution and geolocation for LCZ classification. Next, a set of urban morphology analysis maps were developed. Based on the spatial information supported by the urban morphology analysis maps, land surface properties were classified according to the LCZ classification criteria, and an LCZ classification map was formulated. Finally, spatial distribution pattern of LCZ classes was analyzed, and LCZ datasets were established following the standardized procedure suggested by the LCZ framework. The LCZ classification system not only provides site metadata for UHI observation in Hong Kong, but also expands the global LCZ database under the high-density urban scenario. This study proposes an integrative GIS-based method to process various kinds of planning data for urban morphology analysis and LCZ-based land surface classification, which is also applicable to other cities with a comprehensive set of planning information.

© 2017 Elsevier B.V. All rights reserved.

* Corresponding author at: Room 505, School of Architecture, The Chinese University of Hong Kong, Hong Kong.
E-mail address: zhengyingsheng@link.cuhk.edu.hk (Y. Zheng).

1. Introduction

1.1. Background

The process of urbanization has changed the urban surface structure, resulting in temperature elevation in urban areas. There is an urgent need for optimized urban planning in order to adapt to urban climate change. Although previous urban climate studies have revealed the impacts of urban construction on local climate, the research findings have limited influence on planning practice due to the cross-field barriers between researchers and planners (Ng, 2012; Ren et al., 2011). Climatic researchers are not familiar with the planning process and the different needs of information support at different spatial scales. Likewise, it is hard for planners to understand the complex physical interactions between urban structures and local climate. Hence, interdisciplinary information platforms are needed to bridge the knowledge gaps between different fields. Synergizing various kinds of information in map forms is encouraged, as it presents complex information in an easily understood way for planners, researchers and policy-makers.

To facilitate interdisciplinary knowledge exchange and support metadata for climatic studies, a series of urban classification schemes, e.g. Urban Terrain Zones (UTZ) (Ellefsen, 1991), the Davenport roughness classification (Davenport et al., 2000), and Urban Climate Zone (UCZ) (Oke, 2004), have been developed. However, limitations in climatic relevance, urban-rural representation, nomenclature, origin and scope prevent them from being applied universally. UCZ scheme is the most universal classification among the above classification systems, but more focused on modern and well-developed urban scenarios. Extending the UCZ classification work, the LCZ classification system was introduced by Stewart and Oke (2012) to standardize climatic observations and facilitate worldwide communication on climatic studies. Seventeen basic local climate zones have been identified according to the universally recognized building forms and land cover types. Mapping methods have been successfully integrated into the LCZ classification system, which document and report spatial information in an intuitive way (Bechtel et al., 2015).

Many cities, e.g. Nancy, Toulouse, Bilbao, Glasgow, Uppsala, Phoenix, Nagano, and Vancouver, have applied the LCZ classification system to classify land surface properties and standardize site selection for climatic studies. Houet and Pigeon (2011) have applied the UCZ scheme to classify the urban surface in Toulouse and characterize the associated climatic conditions based on in situ observations and remote sensing data. Leconte et al. (2015) have identified 13 LCZ classes in the Great Nancy Area, where maximum temperature differences over 4 °C among mid-rise zones and low plant zones have been observed. Emmanuel and Krüger (2012) have applied LCZ to the low-density city of Glasgow and examined the influence of urbanization on local climate change using 50 years of historical data. Acero et al. (2013) have employed the LCZ system to classify land surface properties for climate purpose. An LCZ classification map was developed in the study, which provides metadata for site selection and route design of traverse measurements. Middel et al. (2014) used ENVI-met model to simulate the local thermal environment in Phoenix and proposed five neighbourhood design schemes following the LCZ classification system. LCZ application in land surface classification for climate and planning purposes have been discussed in the above studies. However, most of the cities are mainly covered by mid-rise and low-rise buildings, with limited high-rise sample sites. Further tests and applications of LCZ in high-density cities are necessary.

1.2. The need of applying the LCZ classification system in Hong Kong

In the high-density city of Hong Kong, Ng et al. (2012) have developed the Urban Climatic Map (UCMap) system as a climatic information platform to assist decision making for planners and policy makers. The UCMap classifies land surface according to the thermal loads and dynamic potentials of urban morphology. Eight climate classes (“climatopes”) have been identified in Hong Kong. It provides a comprehensive set of planning recommendations at the city and district scales (Ren, 2010).

Comparing to the UCMap system, the LCZ system shares some similarities with the UCMap systems in the identification of land zones with different climatic conditions,

the land surface classification based on a comprehensive set of land cover and urban geometry parameters, and the layered approach to build up the spatial database and formulate the classification map. The main difference between the two systems is the definitions of climatopes and local climate zones. In the UCMap system, climatopes are identified based on the unique topography and climatology of cities. Accordingly, each

city has its unique set of climatopes. In contrast, the classification of local climate zones is universally standardized, which allows cross-city comparison about the climatic conditions and land surface properties (Ng and Ren, 2015). The two systems are mutually beneficial. The LCZ system supports standardized information for the site-specific analysis of the UCMaP system, while the UCMaP system provides inclusive and detailed analysis of local climate conditions.

Given the above, applying the LCZ system into classifying land surface properties and building up the information platform in Hong Kong are necessary. The LCZ classification map may benefit cross-field and cross-city communication. Moreover, the standardized LCZ database could provide site metadata for climatic observations (Lelovics et al., 2014), numerical modeling (Brousse et al., 2016; Ren et al., 2017) and statistical analysis.

1.3. LCZ mapping methods

There are mainly three methods of LCZ classification according to the data sources and analytical methods: manual sampling, remote sensing, and GIS. Since manual sampling is time-consuming and may lead to biased results by different operators, it has not been commonly applied in LCZ mapping at the city level. Remote sensing relies on object-based image analysis or supervised pixel-based classification techniques to develop the LCZ classification map from satellite images (Bechtel and Daneke, 2012). The supervised pixel-based method has been integrated into the World Urban Database and Access Portal Tools (WUDAPT) (Mills et al., 2015). It provides a fast and low-cost way of LCZ classification based on free-access Landsat remote sensing images supported by NASA.

The GIS method is more data-intensive than either the remote sensing method or the manual sampling method, which requires a comprehensive set of planning data. There are two types of GIS method according to the data structure: vector-based method and raster-based method. Vector method has advantages in capturing the shape of objects, as it can follow the exact boundaries of land cover elements. In comparison, raster method is more compatible at geographic scale, and more powerful in statistical analysis for its unified raster grids (Couclelis, 1992). Previous LCZ studies have generally used vector method in mapping local climate zones (LCZs), e.g. in the cities of Szeged and Colombo (Gál et al., 2015; Perera et al., 2012). Considering the purpose of the LCZ classification system for standardizing UHI observations and data documentation, raster method is an appropriate method as it classifies land surface properties and documents spatial data in unified raster grids. Raster method has been successfully employed in developing urban climatic maps, air ventilation maps and urban morphology maps by many previous studies (Ng et al., 2011; Ren et al., 2013).

Local climate zones have uniform surface characteristics, the size of which varies from hundreds to thousands of meters depending on the local surface conditions. In the high-density city of Hong Kong, surface conditions vary considerably within short distances due to the complex urban morphology. Moreover, geolocation of map grids is related to the LCZ classification criteria of building height and building surface fraction, which therefore influence the LCZ classification results. Thus, it also needs to identify an appropriate resolution for raster-based LCZ classification and test the spatial sensitivity LCZ classification results to the geolocation of raster grids.

Considering the research gaps reviewed above, this study aims to: (1) examine the spatial sensitivity of raster-based LCZ classification, (2) classify land surface properties following the LCZ framework, as well as (3) investigate the spatial characteristics of LCZ classification in Hong Kong and establish the LCZ database.

2. Method

2.1. Context

Hong Kong is a high-density city located on the southeast coast of China. It has a total land area of about 1104 km² with hilly and mountainous topography. Around 75% of land in Hong Kong is mountainous area, which is protected as country parks. Only <25% of the land is permitted for urban development (HKPlanningDepartment, 2016b).

Hong Kong has a large population size of around 7.2 Million, with over 90% of the population living in high-rise buildings (Cheung et al., 2005). The highest district population density has exceeded 55,000 persons per



Fig. 1. High-rise and high-density urban morphology in metropolitan areas of Hong Kong.

square kilometer in mid-2014 (HKGovernment, 2015). High population density and limited land resources shape the high-density urban morphology in downtown areas of Hong Kong, associated with densely packed high-rise buildings, deep street canyons, heavy traffic and limited green space (Fig. 1).

2.2. Data

Urban planning information from 2009 has been collected by the Planning Department of Hong Kong. The information includes buildings, streets, topography and land use in GIS format (Ng et al., 2012). Building data is in polygon vector, including the attributes of building footprint and building height. Street data includes street cover data in polygon and street centerline in polyline. Topography data is based on the Digital Elevation Model (DEM) of Hong Kong (in 2 m resolution). Land use data is in 15 m-resolution, containing both urban land use information (commercial, residential, etc.) as well as rural land cover information (woods, shrub, grass, etc.) (HKPlanningDepartment, 2014). Four remote sensing images in the years from 2013 to 2015 (October 5, 2013, December 31, 2013, August 8, 2015, and October 18, 2015) were collected from the US Geological Survey website (<http://glovis.usgs.gov/>) to estimate the vegetation cover conditions and evaluate pervious surface fraction in Hong Kong. The collected datasets were integrated into the GIS platform for sensitivity test, urban morphology analysis and LCZ classification in the following sections.

2.3. Analysis of spatial autocorrelation

Spatial autocorrelation reveals the geographical phenomenon that things closer display more similarity than those further away (ArcGIS, 2011a). This method examines the associations between variance and spatial distance of data, and visualizes the results in semivariograms. In the modeling, semivariance (γ) rises as the spatial distance increases (h), and reaches the maximum level (sill) at the distance of 'range'. In certain circumstances, when γ no longer changes with distance above the 'range', the 'range' is normally recognized as the scale of spatial dependence, i.e. data within the 'range' is spatially correlated with each other.

2.4. Kolmogorov–Smirnov test

Kolmogorov–Smirnov test (K-S test) is a nonparametric test to examine whether two datasets differentiate significantly. The null hypothesis of a two-sample K-S test is that the two samples follow the same distribution pattern. This method has been widely applied in climatic studies to examine the empirical distribution of sample datasets (Knutson et al., 1998; Orłowsky et al., 2008). It has no assumption about the distribution of data, which is applicable for Hong Kong with building height mainly concentrated in high-rise (high-density urban areas) and low-rise (low-density aboriginal settlements) ranges. As the K-S Test requires continuous and one-dimensional datasets, it will be applied in Section 3.2 to determine if different geolocations of the raster grid system influence the statistics of LCZ classification criteria, i.e. building height and building surface fraction, significantly.

2.5. Workflow

There are three main stages of this study: (I). perform sensitivity tests of spatial scale and geolocation of LCZ raster framework, (II). develop a set of urban morphology/land cover analysis maps and the LCZ classification map at city scale, and (III). analyze spatial distribution pattern of LCZ classes and quantify urban morphology characteristics for typical LCZ sites.

In stage I, building data was used to assess the sensitivity of spatial resolution and geolocation of the map grid system. The sensitivity tests identified the optimal spatial scale of Local Climate Zones in Hong Kong, and evaluated the influence of different geolocation of map grids on the LCZ classification results. In stage II, a set of urban morphology analysis maps were developed using the planning data. Based on the urban morphology analysis maps, an LCZ classification map was generated following the LCZ classification criteria. In stage III, the spatial distribution pattern of LCZ classes was evaluated using the LCZ classification map. A set of

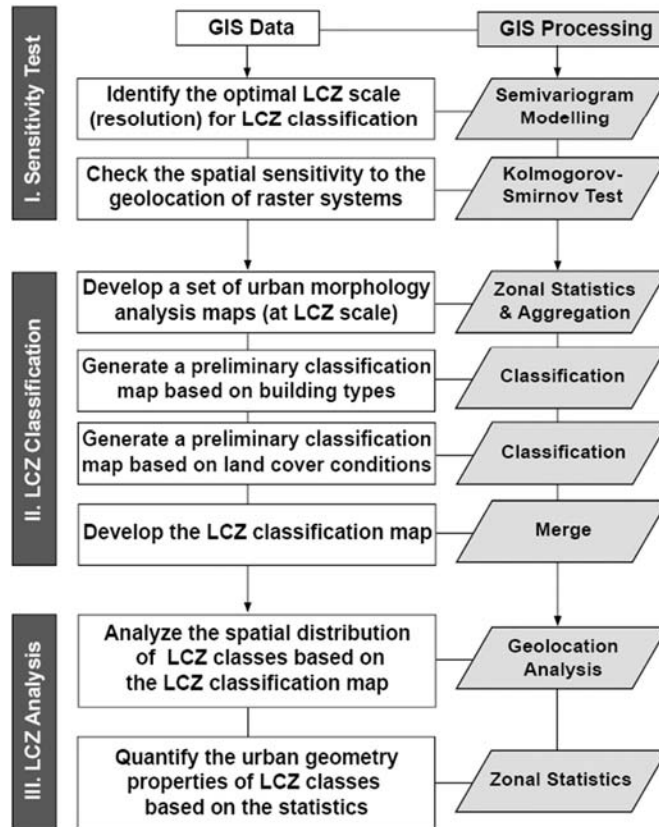


Fig. 2. Workflow of this study.

representative LCZ sites were selected according to the LCZ classification map, based on which the urban geometry properties of LCZs were quantified (Fig. 2).

3. Testing the spatial sensitivity of LCZ classification

3.1. Spatial autocorrelation of building height

In a typical local climate zone with uniform land surface structures, significant spatial autocorrelation exists in urban morphology and land cover conditions. The aim of testing the spatial autocorrelation of urban morphology is to identify the optimal raster resolution for LCZ classification, which is the basis for classifying local climate zones with homogeneous urban morphology. As the semivariogram depicts the spatial autocorrelation of the measured sample points, it is applicable for examining the homogeneity of point-based data (ArcGIS, 2011b). According to the logical division of LCZ, LCZ classes in the building type category are classified according to building height (high-rise, mid-rise, or low-rise) and building surface fraction (compact or open). For the two criteria, building height could be simplified to point-based data based on the geometric center of buildings, while building surface fraction is area-based data with specific site boundaries. Hence, semivariogram modelling was used to test the spatial autocorrelation (homogeneity) of building height. Building surface fraction was not included in semivariogram modelling, as it could not be simplified to point-based data without specified site boundaries (i.e. raster resolution).

The stable semivariogram model of Ordinary Kriging was applied in this study. Fig. 3 shows that semivariance of building height rises as the distance between each two buildings increases, and reaches a

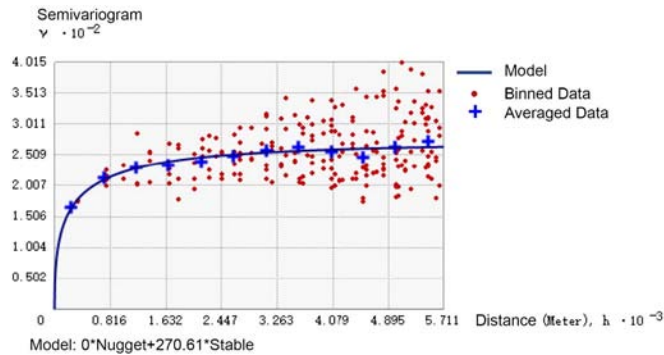


Fig. 3. Semivariogram modelling of building height.

peak level (sill) at a distance (range) around 270 m. Red dots represent binned values and are generated by grouping (binning) empirical semivariogram points. Averaged values are shown as blue crosses and are generated by binning empirical semivariogram points that fall within angular sectors. The results indicate that buildings within 270 m show strong autocorrelation in height, i.e. buildings within 270 m are comparatively homogeneous in height. Considering the climatic sensitivity analysis result of the 300 m grid reported by Lau et al. (2015), and the spatial autocorrelation scale of building height at 270 m, the resolution of raster-based LCZ classification map is determined as 300 m.

3.2. Geolocation sensitivity test of LCZ classification results

Different geolocations of raster grids leads to differentiated building height and building surface fraction, which will influence the classification results (high-rise/mid-rise/low-rise, compact/open). Hence, the Kolmogorov-Smirnov test (K-S test) was used to evaluate whether shifting the raster grids will influence the statistics of building height and building surface fraction significantly. Eight possible shifted directions of grid center point (in 100 m moving distance and 300 m resolution) have been examined: North (N), South (S), West (W), East (E), Northwest (NW), Northeast (NE), Southwest (SW), and Southeast (SE) (Fig. 4). The tests are focused on the built-up urban areas with building surface fraction above 10%. The eight shifted raster maps have been compared with the original raster map in building height and building surface fraction (Fig. 4, Table 1).

The K-S Test results in building height are all zero, which indicates that the null hypothesis is accepted. It means that the frequency distribution of building height follows the same pattern although the location of raster grids changes (Table 1, Fig. 5). Hence, shifting the geolocation of raster grids does not change the classification of high-rise, mid-rise or low-rise classes. However, the test results in building surface fraction show the opposite circumstances. The null hypotheses under all eight categories are rejected, which means that the frequency distribution of building surface fraction changes as the raster grid shifts (Table 1, Fig. 6). The results indicate that building surface fraction is sensitive to the geolocation of raster grids, while building height is not sensitive to that.

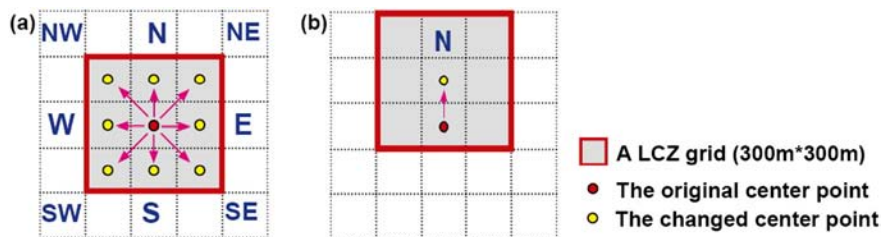


Fig. 4. Nine kinds of different grid geolocation (a) eight shifted directions of grid center point, (b) example of moving grid center point towards north direction.

Table 1

Results of two-sample K-S test at 5% significance level.

		N	S	W	E	NW	NE	SW	SE
Building height	Hypothesis test result	0	0	0	0	0	0	0	0
	P value	0.56	0.84	0.29	0.53	0.56	0.35	0.60	0.45
Building surface fraction	Hypothesis test result	1	1	1	1	1	1	1	1
	P value	0.04	<0.01	0.02	<0.01	<0.01	<0.01	<0.01	<0.01

Given the spatial sensitivity of building surface fraction, preliminary LCZ classification results by the nine raster frameworks were further compared to determine the appropriate raster framework for mapping LCZs. Table 2 reports the number of LCZ grids (LCZ1–LCZ6) in the nine raster frameworks. It shows that the number of grids in each LCZ class varies as the raster framework shifts. The difference between the nine raster frameworks tends to be larger in the LCZs of LCZ1, LCZ4, and LCZ6 with comparatively large sample size. On the whole, the original raster framework has a larger number of grids categorized into the urban LCZs (689 LCZ grids in total) than the other eight shifted raster frameworks. One possible reason is that the eight shifted raster frameworks are associated with higher frequency in building surface fraction below 20%, due to a higher proportion of LCZ grids mixed with non-built-up areas (Fig. 6). It indicates that the original raster may better capture the boundaries of LCZs than the shifted raster frameworks do. On the other hand, the average level of standard deviation of building height in LCZ grids has been calculated to evaluate the homogeneity in building geometry (Table 3). The statistics imply that the original raster framework has comparatively lower standard deviation in building height (especially in high-rise LCZs of LCZ1 and LCZ4) than the other raster frameworks. It implies that the original raster framework performs better in identifying LCZs with uniform building geometry. Given the above, the original raster framework is selected as the spatial reference for classifying LCZs.

4. GIS-based LCZ classification and urban geometric analysis

4.1. Development of land surface analysis maps for LCZ classification

A set of urban morphology analysis maps has been developed based on the planning information in GIS. The maps follow the default/original raster framework with 300 m resolution according to the sensitivity test. The urban morphology analysis maps cover the building geometry parameters of building height (BH), building surface fraction (BSF, i.e. building coverage ratio), sky view factor (SVF) and aspect ratio (H/W); land cover parameters of pervious surface fraction (PSF) and impervious surface fraction (ISF); and street geometry parameter of street width (SW). The definition and calculation methods of the urban morphology parameters at LCZ scale are presented in Fig. 7 and Table 4.

4.1.1. Building height (BH) map

Building height is mean building height of an LCZ grid, weighted with the footprint area of buildings. Mean building height is the key parameter for LCZ classification in urban areas, to identify the high-rise (BH > 25 m), mid-rise (BH = 15–25 m) or low-rise (BH < 15 m) LCZ classes. The building data was first converted into a high-resolution raster map (1 m resolution) according to the building height. Then, the high-resolution building height map was used to calculate mean building height of each LCZ grid (300 m resolution).

4.1.2. Building surface fraction (BSF) map

Building surface fraction is the fraction of land surface covered by buildings. BSF is also the key parameter for differentiating compact (BSF > 0.4) or open (BSF < 0.4) LCZ classes in urban areas. A building cover map in high resolution (1 m) was first developed using the building data. Then, the high-resolution building cover map was aggregated into 300 m resolution, to evaluate building surface fraction at LCZ scale.

4.1.3. Sky view factor (SVF) map

The SVF calculation tool in SAGA GIS (Conrad et al., 2015) was first applied to develop a high-resolution SVF map (in 2 m resolution) for an entire land surface area of Hong Kong. The input data for the SVF calculation in SAGA GIS was a Digital Surface Model (DSM), which contains elevations of both natural features such

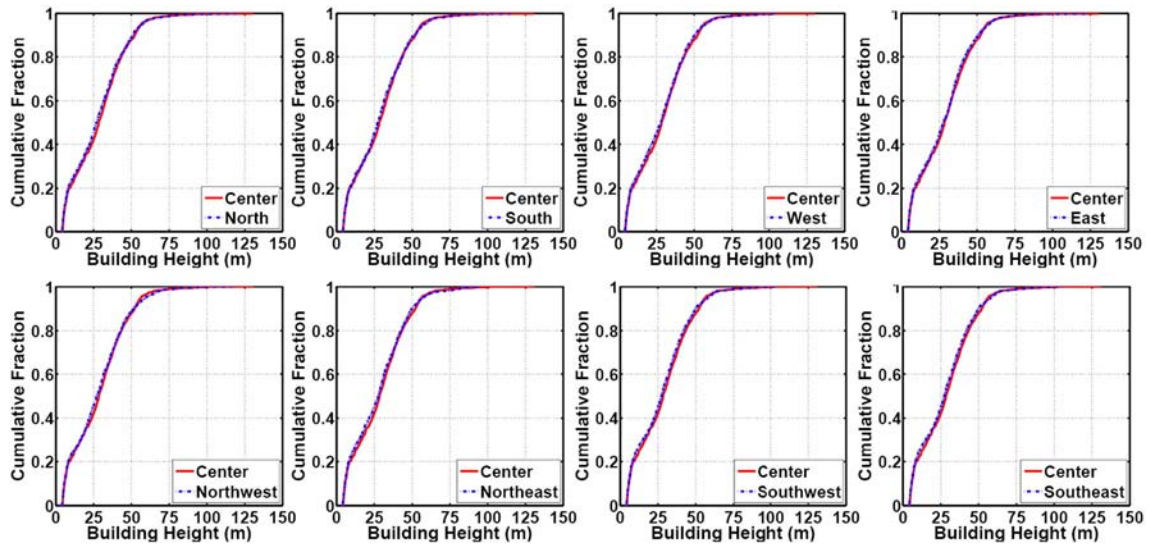


Fig. 5. Comparison of the original raster framework with eight shifted raster frameworks in the cumulative fraction of building height.

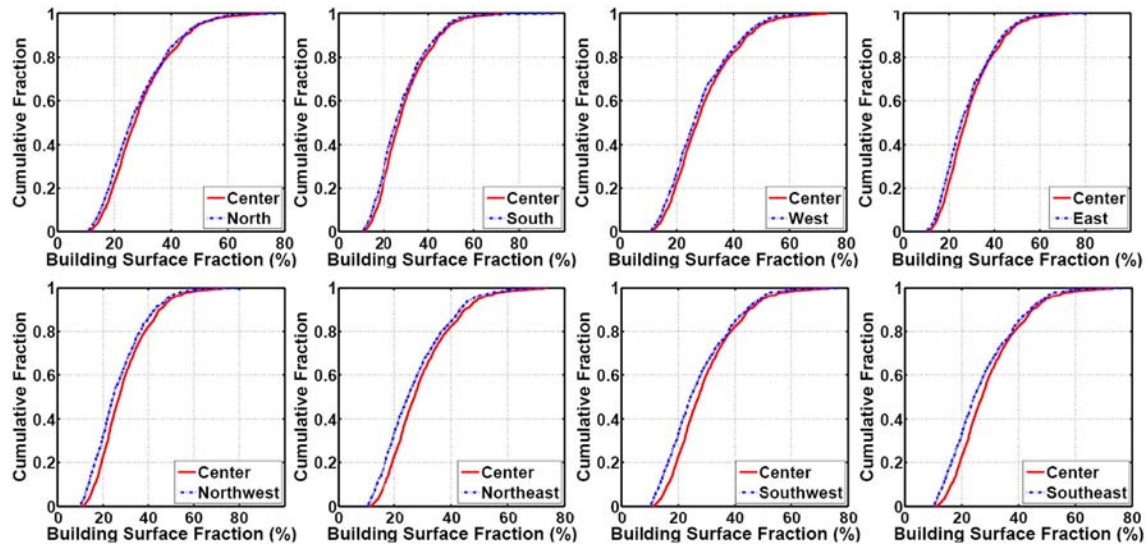


Fig. 6. Comparison of the original raster framework with eight shifted raster frameworks in the cumulative fraction of building surface fraction.

Table 2

Number of LCZ grids in LCZ1–LCZ6 using the nine raster frameworks (original, N, S, W, E, NW, NE, SW and SE).

Number of LCZ grids	Original raster framework	Shifted raster frameworks								
		N	S	W	E	NW	NE	SW	SE	
LCZ1	139	133	128	123	131	136	127	124	126	
LCZ2	14	19	15	19	15	10	16	17	13	
LCZ3	6	5	9	6	6	7	5	8	4	
LCZ4	317	295	280	283	279	263	278	275	255	
LCZ5	89	90	85	87	96	81	94	74	92	
LCZ6	124	119	122	125	118	105	106	110	96	
Sum	689	661	639	643	645	602	626	608	586	

as mountains and rivers in addition to man-made features such as buildings. Second, the high-resolution SVF map was used to extract the SVF values at ground level, which excludes the SVF values on top of buildings. Lastly, the SVF map at ground level was used to calculate mean SVF of each LCZ grid and formulate the mean SVF map (300 m resolution) via the aggregation technique in GIS.

4.1.4. Aspect ratio/height width ratio (H/W) map

Aspect ratio is defined as the ratio of height to width of a street canyon, which has been widely discussed at street level by previous studies (Ali-Toudert & Mayer, 2006; Santamouris et al., 1999). However, calculation of aspect ratio is difficult in Hong Kong, due to the complex street geometry: (1) building height and street width (determined by building setback) variate inside the same street, and (2) high-rise buildings mostly consist of towers and podiums, which result in different setbacks from the streets at the vertical level and step-shaped street canyons (Ng et al., 2011). Given the complex street geometry, there is no standardized way in the calculation of aspect ratio (HKBuildingDepartment, 2009; Houet and Pigeon, 2011). This study adopted the method recommended by the Sustainable Building Design Guidelines in Hong Kong (HKBuildingDepartment, 2009). The mean aspect ratio of an LCZ grid (300 m) was calculated using the area-weighted mean building height divided by the mean street width through raster calculation in GIS. Mean street width was computed by the total street area divided by the total street length in an LCZ grid.

4.1.5. Pervious surface fraction (PSF) map

Pervious surface is mainly composed of vegetation and waterbody, which is helpful for moderating urban heat island via evaporation (Xu, 2009). Pervious surface fraction, defined as the fraction of pervious surface in an LCZ site, is an important parameter related to UHI development at local scale. In this study, PSF was calculated as the sum coverage ratio of waterbody and vegetation in an LCZ grid. The coverage ratio of waterbody was evaluated using the planning data of waterbody containing rivers, reservoirs and coasts, while the coverage ratio of vegetation cover was estimated based on remote sensing images.

The remote sensing images collected from the US Geological Survey website were used to calculate Normalized Difference Vegetation Index (NDVI) and generate the NDVI map in Hong Kong according to the

Table 3

Standard deviation of building height in LCZ grids (average level of LCZ1–LCZ6).

Standard deviation	Original raster framework	Shifted raster frameworks								
		N	S	W	E	NW	NE	SW	SE	
LCZ1	34.39	34.61	34.90	33.79	36.08	34.60	34.62	35.00	34.89	
LCZ2	14.41	14.88	18.77	16.82	14.80	17.77	15.50	17.22	16.01	
LCZ3	4.29	2.33	4.68	5.24	8.31	3.44	3.06	6.57	12.19	
LCZ4	33.79	34.45	34.52	34.84	33.68	34.51	34.01	34.27	35.07	
LCZ5	16.77	18.63	18.14	18.50	18.59	18.80	19.06	18.89	18.59	
LCZ6	4.02	4.56	3.79	4.51	4.54	4.30	4.40	4.04	4.53	

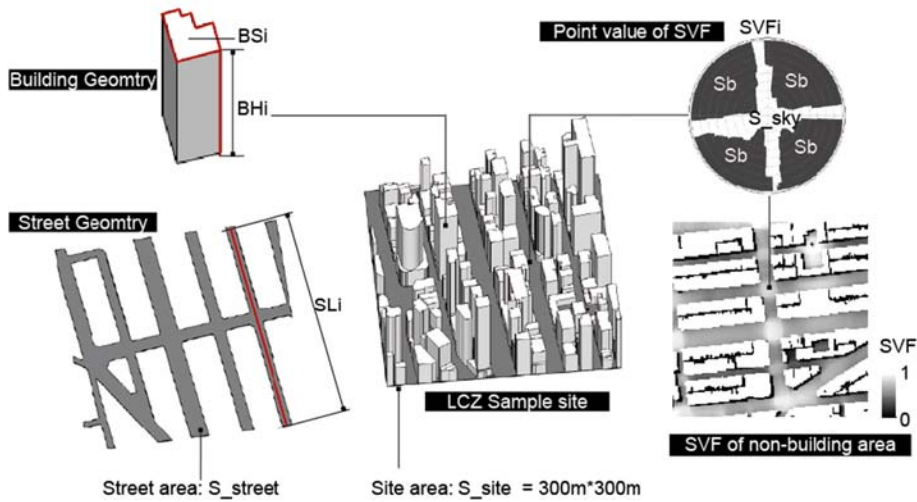


Fig. 7. Urban morphology parameters calculation.

Table 4

Definition and calculation methods of urban morphology parameters.

Parameters	Definition	Basic data	Calculation methods
BH	Area-weighted mean building height of the sample site. n is the number of buildings of the LCZ sample site. BSi is the ground area of a building. BHi is the height of a building. $\sum_{i=1}^n BSi \cdot BHi$ is the total building volume of the site. $\sum_{i=1}^n BSi$ is the total building cover area of the site.	Building data	$BH = \frac{\sum_{i=1}^n BSi \cdot BHi}{\sum_{i=1}^n BSi}$
BSF	Building surface fraction, i.e. building coverage ratio of the sample site. n is the number of buildings of the LCZ sample site. S_site is the total area of the site.	Building data	$BSF = \frac{\sum_{i=1}^n BSi}{S_site}$
SVF	Areal mean SVF of non-building areas of the sample site (Chen et al., 2010). $SVFi$ is the SVF value of a certain point in non-building area (point area $1\text{ m} \times 1\text{ m}$) in the LCZ sample site. n is the number of SVF points ($1\text{ m} \times 1\text{ m}$) in non-building area of the site. S_Sky and $\sum Sb$ represent the area of sky and the area occupied by buildings in a certain point respectively. $S_Sky + \sum Sb$ represents the entire hemispheric environment in a certain point.	Building and topography data	$SVF = \frac{\sum_{i=1}^n SVFi}{n}$ $SVFi = \frac{S_Sky}{(S_Sky + \sum Sb)}$
H/W	Areal mean aspect ratio of sample sites. It is defined as the ratio of mean building height to mean street width in the LCZ sample site.	Building and street data	$H/W = \frac{BH}{SW}$
PSF	Pervious surface fraction of the LCZ sample site. $\sum S_per$ is the total area of pervious surface, with NDVI above 0.2 (Weier and Herring, 2000)	Remote sensing data	$PSF = \frac{\sum S_per}{S_site}$
ISF	Impervious surface fraction of the LCZ sample site.	Building and remote sensing data	$ISF = 1 - BSF - PSF$
SW	Mean street width of sample sites. n is the number of streets in the LCZ sample site. $\sum S_street$ is the total area of streets in the site. $\sum_{i=1}^n SLi$ is the total length of streets in the site.	Street data	$SW = \frac{\sum S_street}{\sum_{i=1}^n SLi}$

following equation (Liu and Zhang, 2011).

$$\text{NDVI} = \frac{\text{NIR} - R}{\text{NIR} + R}$$

According to the publication of NASA, vegetation is associated with NDVI values above 0.2 (Weier and Herring, 2000). Hence, the vegetation cover map in Hong Kong was developed based on the NDVI map, with NDVI values above 0.2.

4.1.6. Impervious surface fraction (ISF) map

Due to the intense urban development in urban areas of Hong Kong, most of the urban land surface is covered by impervious surface such as buildings and roads. Impervious surface fraction of an LCZ grid is defined as the fraction of paved surface outside buildings (Stewart, 2011). Thus, the impervious surface fraction map was formulated following the formula: $\text{ISF} = 1 - (\text{BSF} + \text{PSF})$ (Unger et al., 2014).

4.1.7. Land use (LU) map

The proportion of different land use type in each LCZ grid was computed using the land use data, based on which the dominant land use type for each LCZ grid has been identified. For LCZ grids not classified according to the building-type classification, they were classified according to the land cover type based on the LU map.

4.2. LCZ classification based on the land surface analysis maps

The land surface analysis maps at LCZ scale were further used to develop the LCZ classification map in Hong Kong. First, the BH map and BSF map were used to identify the building-type LCZ classes. There are seven building-type LCZ classes identified according to the building height levels (high-rise/mid-rise/low-rise) and the building compactness (compact/open) (Stewart and Oke, 2012). The definition and classification criteria of LCZ classes could be referred to Fig. 12 and Table 7 in Appendix. Second, the land surface areas not categorized in building-type LCZ classes in the first step, were further examined based on the LU map. As introduced in Section 4.1, the LU map reveals the dominant land cover type for LCZ grids. Hence, seven land cover types have been classified according to the dominant land cover types. Third, the classification of building types in step one and the classification of land cover types in step two were spatially merged to generate the LCZ classification map. LCZ types in some of the LCZ grids were manually updated, according to the planning schemes (HKPlanningDepartment, 2016a) and land cover information from Google maps. The spatial information of LCZ grids in building height, building surface fraction, sky view factor, aspect ratio, pervious surface fraction, and impervious surface fraction were supported by the BH map, BSF map, SVF map, H/W map, PSF map, and ISF map. The spatial information was associated with the LCZ grids in the LCZ classification map to build up the LCZ database in Hong Kong. The workflow of LCZ classification based on planning data is summarized in Fig. 8.

4.2.1. LCZ classification based on building forms

The seven LCZs classified by building types include Compact High-rise (LCZ1), Compact Mid-rise (LCZ2), Compact Low-rise (LCZ3), Open High-rise (LCZ4), Open Mid-rise (LCZ5), Open Low-rise (LCZ6), and Sparsely Built (LCZ9). Lightweight Low-rise (LCZ7), Large Low-rise (LCZ8) and Heavy Industry (LCZ10) were not found in Hong Kong.

4.2.2. LCZ classification based on land cover types

Land use of woodland and mangrove were classified to the tree class (LCZA & LCZB). Due to the lack of tree geometry information, it was not possible to differentiate LCZA and LCZB. Land use of shrubland was categorized as LCZC, while grassland and agricultural land were classified as LCZD. Roads, airports, container terminals, bad lands and quarries were categorized as LCZE. Seashore and bare soil were assigned to LCZF. Fish ponds, reservoirs, streams and nullahs were categorized as LCZG. Mudflat was assigned to LCZW.

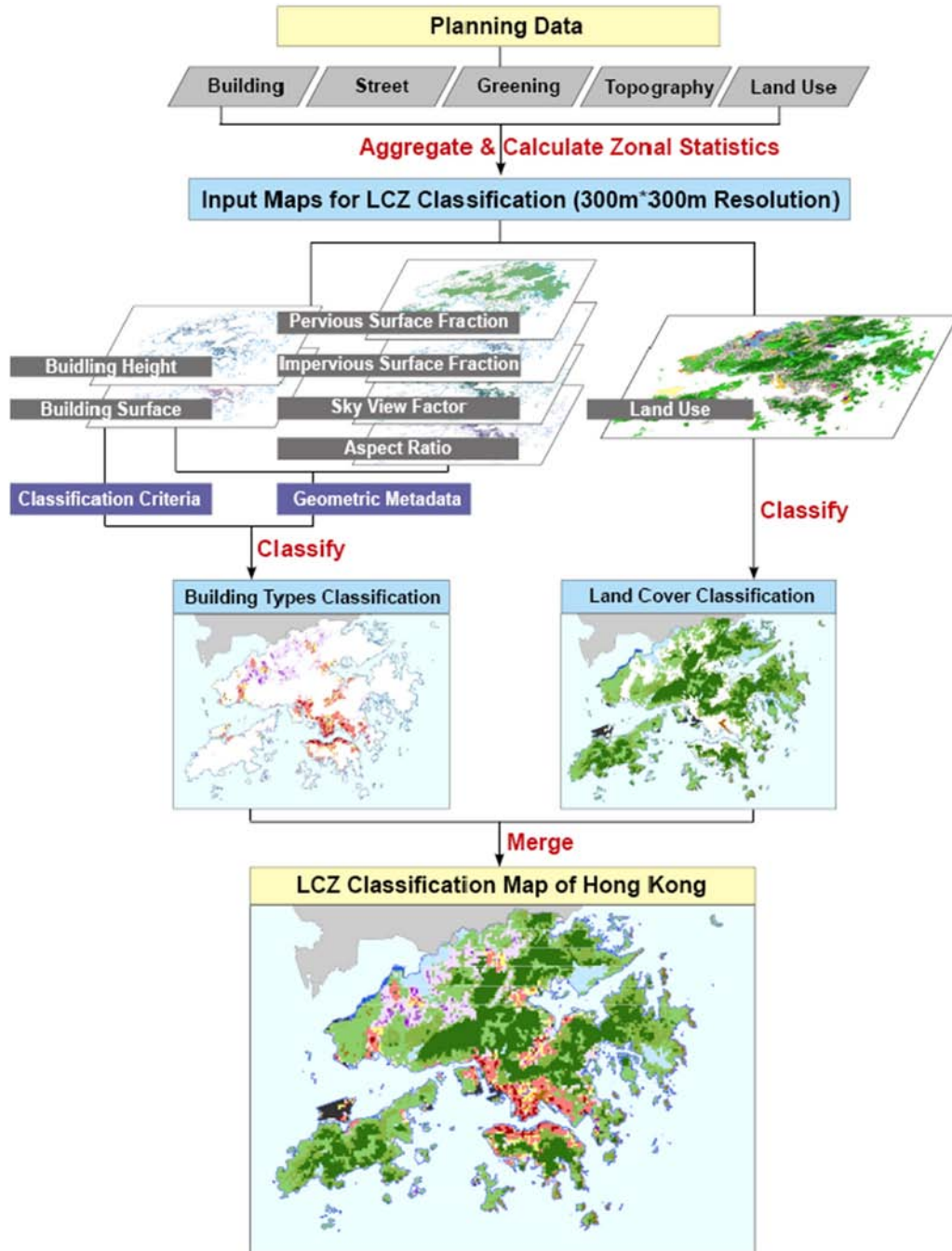


Fig. 8. Flow chart of developing LCZ classification map of Hong Kong.

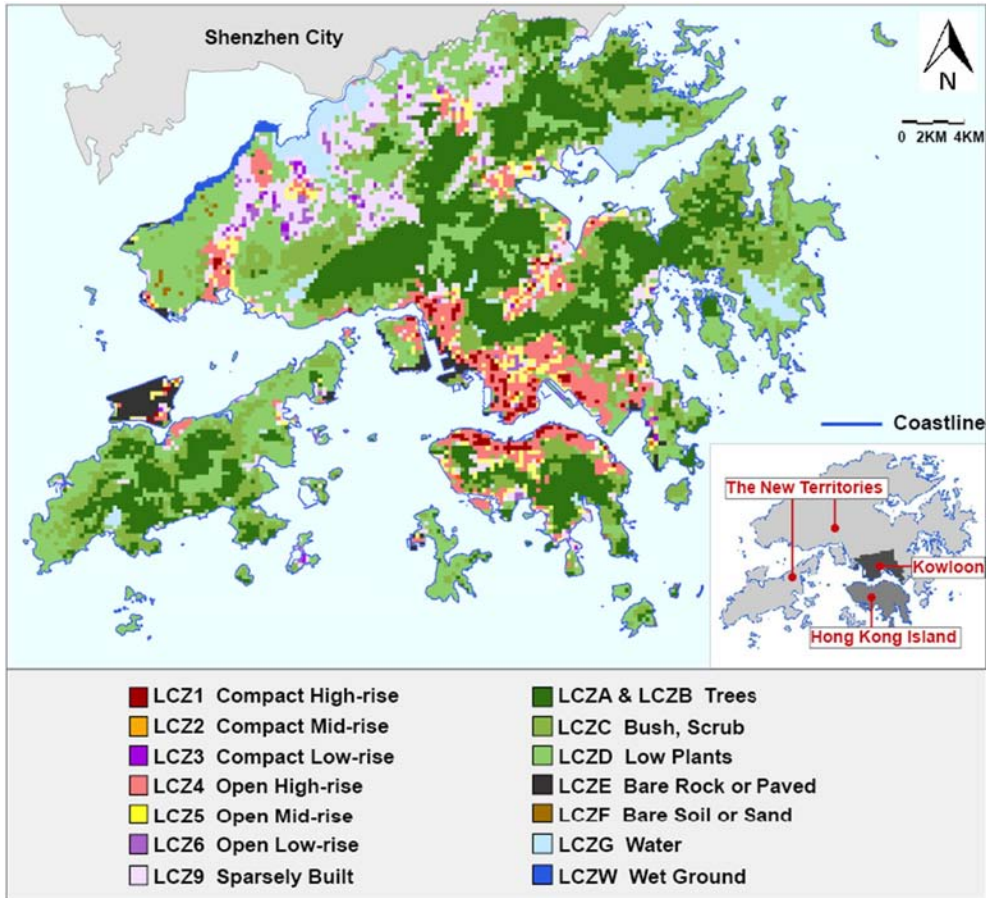


Fig. 9. LCZ classification map of Hong Kong.

4.3. Spatial distribution pattern of LCZs in Hong Kong

As the LCZ classification map shows, land surface conditions in Hong Kong demonstrate significant diversity in land cover types and building types (Fig. 9). The large land surface of Hong Kong is covered by the vegetated LCZs of LCZA–LCZD, mainly located in the New Territories and the southern part of Hong Kong Island. LCZE consists of container terminals, airport runways and quarries, which are mainly distributed in the coastal areas of the New Territories. LCZF mainly includes sandy seashores, distributed along the eastern coastline. Large water bodies (LCZG), such as fish ponds, reservoirs, and lakes are primarily located in the north and east part of the New Territories. Wetland along the northwest coast of the New Territories was classified as LCZW.

In the highly-urbanized areas of Kowloon, the northern part of Hong Kong Island, as well as city centers in the New Territories, the dominant LCZs are high-rise classes of LCZ1 and LCZ4. This is the reason why Hong Kong is recognized as a high-rise and high-density city although over three-quarters of land is protected as non-urbanized country parks. Samples of LCZ2 are limited, sparsely distributed in the old town areas of Kowloon and the New Territories. LCZ5 generally appears on the periphery of high-rise LCZ clusters. Distribution of low-rise LCZs (LCZ3, LCZ6 and LCZ9) in Kowloon and Hong Kong Island is limited, with small samples gathered in the areas away from the coastline. In contrast, large urban areas of the northwest of the New Territories are dominantly covered by low-rise LCZs, mixed with high-rise LCZs clusters in the city centers. Moreover, some fishing villages, categorized as LCZ9, are scattered in the coastal areas.

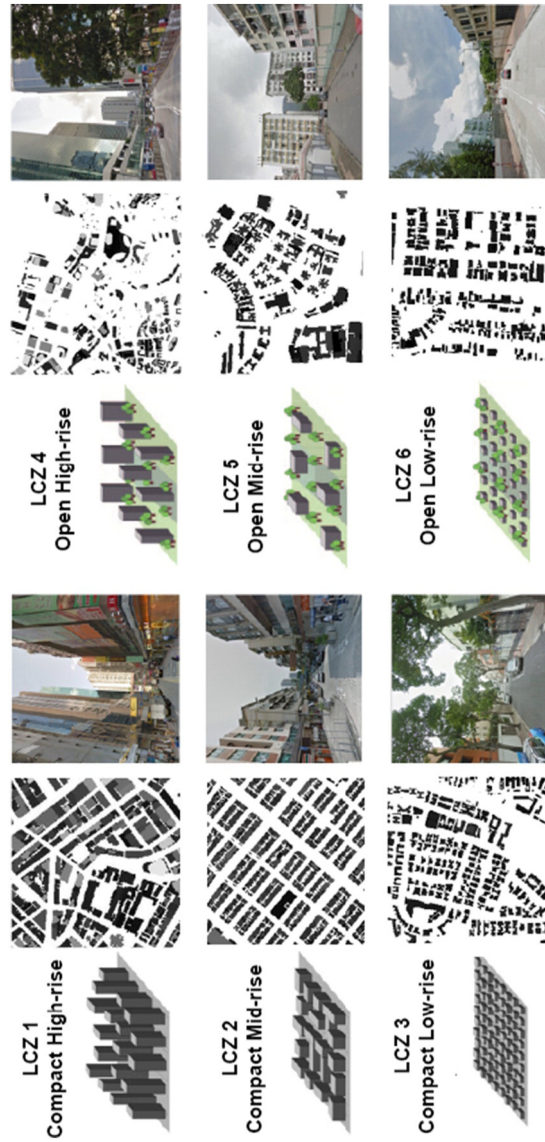


Fig. 10. Samples of LCZ1–LCZ6 in Hong Kong.

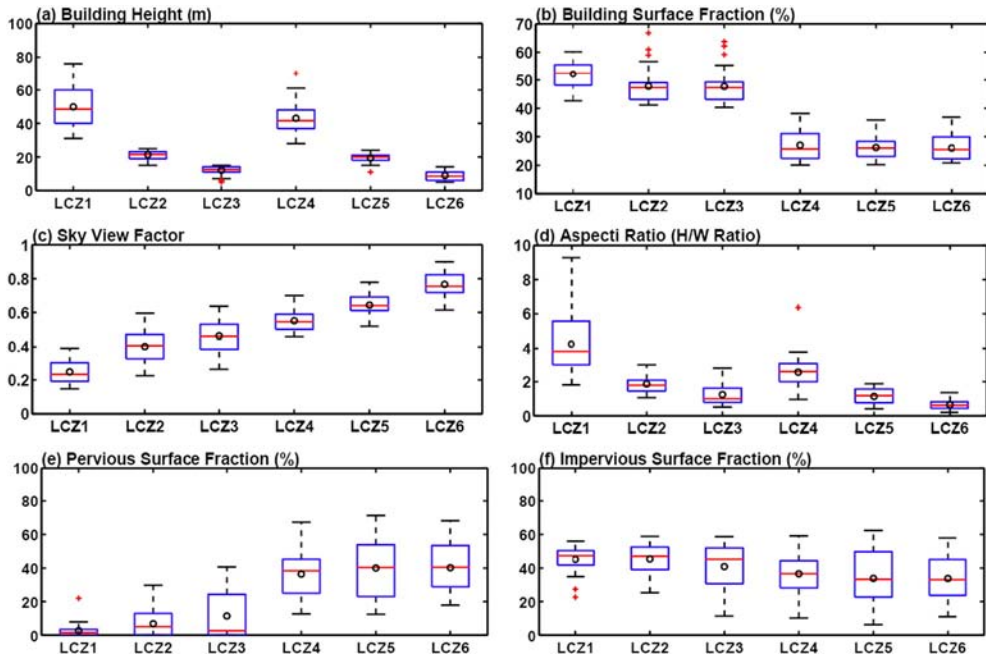


Fig. 11. Boxplot of urban geometry parameters of LCZ sample sites.

4.4. Urban geometric properties of LCZs

To quantify the urban geometric properties of LCZs (focused on LCZ1-LCZ6) under the high-density urban scenario of Hong Kong, a set of typical sample sites of LCZ1-LCZ6 have been selected and analyzed based on the LCZ classification map and land surface analysis maps. Selecting typical sample sites for describing the LCZ characteristics in Hong Kong is necessary, as raster grids could not precisely describe the boundaries of land surface features such as roads, rivers, mountains, etc. Hence, visual interpretation was used to check the shape, size, texture, and agglomeration patterns of land surface elements (i.e. buildings, roads and urban blocks etc.) in the LCZ grids aided by the planning information. A set of typical LCZ grids with comparatively homogeneous urban forms was identified (Fig. 10), in line with the representative examples shown in the study of Stewart and Oke (2012).

The statistics of the urban morphology parameter are reported in Fig. 11 and Table 5. The results are basically consistent with the LCZ statistics documented by Stewart and Oke (2012), apart from some differences in

Table 5
Statistics of urban morphology parameters of LCZ sample sites.

LCZ classes	Sky view factor (SVF)	Areal aspect ratio (H/W)	Building surface fraction (BSF)	Impervious surface fraction (ISF)	Pervious surface fraction (PSF)	Height of roughness elements (BH)	Terrain roughness class ^a	Percentage of occurrence (%)
LCZ 1	0.1–0.4	2–10	40–70	30–60	<10	>25	8	8.7
LCZ 2	0.2–0.6	1–3	40–70	20–60	<30	15–25	6–7	1.0
LCZ 3	0.2–0.6	0.5–3	40–70	10–60	<50	5–15	6	2.2
LCZ 4	0.4–0.7	1.5–4	20–40	10–60	10–70	>25	7–8	54.8
LCZ 5	0.4–0.8	0.5–2	20–40	10–60	10–70	15–25	5–6	24.6
LCZ 6	0.6–0.9	0.2–2	20–40	10–60	10–70	5–15	5–6	8.7

^a Davenport et al.'s classification of effective terrain roughness (z_0) for city and country landscapes (Davenport et al., 2000).

the LCZs of Compact High-rise zones (LCZ1), Compact Mid-rise (LCZ2) zones, and Compact Low-rise zones (LCZ1-LCZ3). Standardized datasheets are attached in the Appendix (Figs. 13–18). The main differences lie in the parameters of SVF, H/W, and PSF, which have been widely identified as the key indicators of UHI intensity at local scale (Chang and Goh, 1999; Hart and Sailor, 2009).

Negative proportional correlations between SVF and UHI intensity during night-time have been observed in previous studies (Svensson, 2004; Unger, 2004). Low SVF is associated with limited exposure to open sky, and accordingly, results in a weakened process of radiative/convective cooling. It indicates that UHI intensity tends to increase as SVF decreases. SVF values in the compact zones (LCZ1-LCZ3, SVF = 0.1–0.6) are comparatively lower than those in the open zones (LCZ4-LCZ6, SVF = 0.4–0.9), primarily due to the densely packed buildings (Table 5). The SVF values of LCZs in Hong Kong are comparatively lower than those of other cities (Stewart, 2011), particularly for the Compact High-rise zones. There are some sites of LCZ1 in Hong Kong with SVF values even below 0.2, the minimum SVF in Compact High-rise zones recorded by Stewart. The LCZ1 samples with low SVF values in Hong Kong are generally associated with compact high-rise buildings, intense human activities, and heavy industry, where UHI mitigation measures are highly needed.

Aspect ratio is a key parameter for describing urban canyon geometry and local climate conditions (Memon et al., 2010; Oke, 1981). Oke (1981) has demonstrated that the increase of aspect ratio contributes to the elevation of daily maximum UHI intensity, as it impedes the long-wave radiative heat loss. Chang and Goh (1999) have found that aspect ratio of urban canyons in Singapore is positively correlated with nocturnal UHI intensity in the residential estates of Singapore. Table 5 shows that the compact LCZs in Hong Kong have higher aspect ratio than the open ones. High-rise LCZs demonstrate wider range of aspect ratio than the mid-rise and low-rise zones due to the variation in height of tall buildings. Certain compact high-rise samples (LCZ1) have aspect ratios up to 10, while mid-rise and low-rise samples generally have the corresponding values below 3.

Vegetated area is a primary component for pervious surface in Hong Kong. Pervious surface fraction (PSF) mainly reveals the vegetation coverage ratio of LCZ sites. Cooling effects of vegetation on the surrounding urban areas have been widely identified by previous studies (Chow et al., 2011; Spronken-Smith and Oke, 1998). The cooling effect is strong during night, which is fed by the outgoing net radiation by the thermal heat flux as well as latent heat flux through evaporation and transpiration (Wong and Yu, 2005). The influence can be extended from the borders of vegetated areas to the surrounding urban environment through air advection (Upmanis and Chen, 1999). According to the statistics in Table 5, the compact LCZs have comparatively low PSF because of the high coverage ratio of buildings. The open LCZs have more non-building area, and accordingly show wide variation in PSF (Table 6). LCZ1 has the lowest PSF (below 10%) among the six LCZs, whereas the open LCZs of LCZ3-LCZ6 could have the PSF up to 70%.

5. Discussion

5.1. GIS-based LCZ classification method

There are few previous studies using a GIS-based method in developing LCZ classification maps at city level, owing to the planning data availability. The vector method has been used as the main method in previous studies for GIS-based mapping of LCZs, e.g. in Szeged and Colombo (Gál et al., 2015; Perera et al., 2012). In Szeged, plots were firstly classified according to the criteria of LCZs. The classified plots were further aggregated into groups, based on a set of aggregation rules according to the identity, similarity, and proximity of

Table 6
Standard deviation of urban geometry parameters of LCZ sample sites.

LCZ classes	Sky view factor (SVF)	Areal aspect ratio (H/W)	Building surface fraction (BSF)	Impervious surface fraction (ISF)	Pervious surface fraction (PSF)	Height of roughness elements (BH)
LCZ 1	0.07	1.76	0.06	0.07	0.03	12.72
LCZ 2	0.10	0.50	0.06	0.10	0.07	2.51
LCZ 3	0.11	0.61	0.06	0.15	0.16	2.45
LCZ 4	0.07	1.04	0.05	0.09	0.11	9.84
LCZ 5	0.07	0.43	0.04	0.13	0.15	2.66
LCZ 6	0.07	0.28	0.04	0.11	0.11	2.90

plots. Then, the aggregated groups were generalized into local climate zones through the post-classification filtering, with a control of the minimum size as 500 m. In Colombo, Perera et al. (2012) classified the surface properties of plots using the similar method in Szeged.

Different from the two-step processing of LCZ classification and generalization using the vector method, the raster method gives a simultaneous processing of the LCZ classification and generalization. This study proposes a workflow for raster-based LCZ classification. In this study, vector data (e.g. building, street data) has been converted to high-resolution raster data to minimize the error introduced by vector-raster conversion. Based on the high-resolution raster data, a set of urban morphology analysis maps have been generated with LCZ grid size as 300 m. Through the spatial statistics supported by the urban morphology analysis maps, each raster grid has been given an LCZ identity associated with a comprehensive set of urban morphology metadata. The grid groups with the same LCZ identity are considered as local climate zones.

Compared to the vector-based method, the raster-based method is also helpful for classifying LCZs and building up the LCZ database for several reasons. First, the raster-based method provides a standardized spatial grid system for synergizing multiple layers of data. Second, the statistics in different raster grids are directly comparable due to the unified grid size. Third, the raster-based classification map may provide a reference for sample site selection with an exact size control. However, the regular grid is also the main limitation of the raster method, which cannot follow the natural boundaries of LCZs. Therefore, a sensitivity test for resolution and geolocation of raster frameworks is critical for getting a reliable LCZ classification result.

5.2. Spatial sensitivity of LCZ classification

Semivariogram modeling was applied to select the appropriate resolution for the LCZ classification map in this study. The results indicate that buildings within a distance of 270 m in Hong Kong are spatially autocorrelated. In other words, buildings within a distance of 270 m are at similar height level. This finding is consistent with the conclusion in previous climatic mapping studies in Hong Kong. Lau et al. (2015) have examined the climatic sensitivity of different grid sizes in 200 m, 300 m, 400 m and 500 m based on a set of LCZ sample sites in Hong Kong. According to the results, the strongest correlation between climatic parameters (air temperature and relative humidity) and urban morphological parameters have been found in 300 m grid size. Chen et al. (2010) have found that SVF calculated at 300 m diameter can best explain the intra-urban temperature variation in high-density urban areas of Hong Kong. Ng et al. (2011) have also identified that the frontal area density statistics in 300 m grid shows the best performance in predicting local wind environment in high-density urban areas of Hong Kong.

Spatial sensitivity tests are necessary not only for the raster-based method but also for the vector-based LCZ classification. The post-classification filtering procedure results in a larger size and a smaller number of local climate zones, which presents a more generalized but less varied spatial pattern. Gál et al. (2015) have pointed out that post-classification filtering may lead to the disappearance of some land surface elements from the map. Hence, determining the appropriate size for post-classification filtering based on the vector method is important, to achieve a balance between generality and local variability.

Previous studies have reported different LCZ sizes in different cities based on the manual sampling method, e.g. 250 m radius for Toulouse (Houet and Pigeon, 2011), 100 m radius for the central areas of Nagano and Uppsala, 200 m radius for Vancouver (Stewart et al., 2014), as well as 200 m for Nancy (Leconte et al., 2015). The findings of the above studies indicate that the optimal size of LCZs may vary across cities, and it is necessary to perform sensitivity test of LCZ sizes for different cities.

This study has also examined the influence of the geolocation of raster frameworks on LCZ classification results, which has received little attention before. The Kolmogorov-Smirnov Test results indicate that shifting the raster framework changes the frequency distribution pattern of building surface fraction, and accordingly, influences the LCZ classification results. Through comparisons of the number of classified LCZ grids and the average standard deviation in each LCZ class (in LCZ1–LCZ6), the original raster framework shows the best performance in identifying LCZ grids with uniform building geometry.

5.3. LCZ application in land surface description and communication for UHI studies

The LCZ classification system provides a comprehensive framework for describing land surface properties, which documents site metadata in a standardized way for climatic studies. The LCZ map gives an intuitive

interpretation of local climate conditions at city scale, while the LCZ database supports quantitative information about geometric, land cover and radiative properties. The LCZ system gives a general and simplified climatic context at city level, as on-site measurement or numerical simulation of a whole city are excessively data-intensive. Moreover, the system provides a spatial reference about the distribution of critical areas for UHI observation and mitigation. The initial results of this study have been used to select sample sites for urban heat island monitoring in Hong Kong (Zheng, 2016; Zheng et al., 2015). Lelovics et al. (2014) have applied the LCZ system to select representative sites and establish a UHI monitoring network in Szeged. Leconte et al. (2015) have classified land surface properties of Nancy following the LCZ system, and performed mobile traverse measurements to examine the local climatic conditions in LCZ classes.

Moreover, the LCZ classification system allows worldwide communication of UHI studies as the LCZ classes are classified according to the universally recognized building forms and land cover types rather than local surface properties in certain cities. The LCZ map and LCZ database in Hong Kong expand the global LCZ database under high-density scenario, which enables comparison and communication with other cities such as Szeged in Hungary (Unger et al., 2014), Bilbao in Spain (Acero et al., 2013), Colombo in Sri Lanka (Perera et al., 2012), Wuhan and Hangzhou in China (Ren et al., 2016), where spatial database of LCZ at city level has been established.

The dominant LCZ type in the urban areas of Szeged is LCZ6, Open Low-rise. In the city center, the dominant type is LCZ2 Compact Mid-rise. The primary LCZ types in Bilbao are LCZ5 Open Mid-rise and LCZ6 Open High-rise with the total occurrence frequency around 50%. There is also a large sample size of LCZ2 Compact Mid-rise, with an occurrence frequency of 17%, mainly distributed in the central areas near the river. In Colombo, most of the city is covered by LCZ3 Compact Low-rise (48%), and a significant percentage falls in LCZ8 Large Low-rise (24%). The above cities are generally in low density dominated by mid-rise and low-rise LCZ classes, with limited high-rise LCZ samples.

In China, high-rise LCZ classes are the major forms for new town developments in high-density cities, primarily due to the limited land resources and high population density. In Wuhan, the old downtown areas are mainly covered by LCZ4 Open High-rise and LCZ3 Compact Low-rise, while the new town areas are mostly classified as LCZ5 Open Mid-rise and LCZ3 Compact Low-rise. In Hangzhou, large urban areas are densely covered by LCZ1-LCZ4, which experiences a higher density level than Wuhan. According to the LCZ statistics in Hong Kong, the dominant LCZ types are LCZ4 Open High-rise (54.8%) and LCZ5 Open Mid-rise (24.6%). LCZ1 Compact High-rise shows a significant coverage ratio (8.7%), and is highly concentrated in the central urban areas such as northern Hong Kong Island and Kowloon Peninsula. Moreover, there is a large sample size of LCZ6 Open Low-rise, mainly distributed in the peripheral areas.

5.4. LCZ application in climatic planning

This study has established a workflow of raster-based LCZ classification in Hong Kong. It has illustrated the procedures of processing multiple planning information into standardized urban morphology analysis maps, and classifying land surface properties based on the urban morphology analysis maps. This method is also applicable to other cities with high-resolution planning information.

The urban morphology analysis maps and the LCZ classification map are the core results of this study. The LCZ classification map provides an overview of urban forms and land cover conditions in Hong Kong, which may assist planners in identifying critical areas for UHI mitigation. The urban morphology analysis maps provide urban morphology statistics at LCZ scale, which allows powerful meta-analysis for climatic analysis. Zheng (2016) has introduced the potential of applying the LCZ classification system into Outline Zoning Plans (OZP) for UHI mitigation in Hong Kong. The occurrence frequency of urban LCZ classes (LCZ1-LCZ6) in each OZP area has been quantified, based on which a set of planning strategies at OZP level has been proposed. It has highlighted that the OZP areas in Hong Kong Island and Kowloon Peninsula, which are mainly covered by LCZ1, are critical areas for planning optimization and UHI mitigation.

6. Conclusion

This study proposes an integrative GIS-based method of LCZ classification. Spatial sensitivity of LCZ classification has been examined to determine the appropriate raster framework for mapping. A set of urban

morphology analysis maps has been generated as meta-data, based on which the LCZ classification map has been developed.

The key findings of this study are summarized as follows: (1) The optimal LCZ size/resolution for LCZ classification in urban areas of Hong Kong is around 300 m. Building surface fraction is sensitive to the geolocation of raster grids, while building height is not. Hence, spatial sensitivity test is necessary for developing LCZ classification maps. (2) The LCZ classification system is applicable in Hong Kong, to classify and describe the land surface properties. Land surface conditions in Hong Kong show diversity in building types and land cover types, and a total of 15 LCZ classes has been identified. (3) The large land surface of Hong Kong is covered by the vegetated LCZs of LCZA–LCZD. However, high-rise LCZs are the dominant types in urban areas. The urban morphology statistics of LCZ1–LCZ6 are basically consistent with those documented by Stewart and Oke (2012), apart from some differences in sky view factor, aspect ratio, and pervious surface fraction. (4) The urban morphology analysis maps and the LCZ classification map are the core results of this study, which provide standardized spatial information for UHI studies and planning decision making.

Acknowledgements

The study is supported by the Postgraduate Studentship (PGS) 1155045085/PHD/ARK from the Chinese University of Hong Kong and an Early Career Scheme Project Grant 2013/14 (Project No.: RGC-ECS458413, named “Applying “Local Climate Zone (LCZ)” into High-density High-rise Cities – A Case Study in Hong Kong”) of Hong Kong Research Grants Council. The authors wish to thank Dr. Iain Stewart, Prof. Gerald Mills and Dr. Yuan Shi for the valuable suggestions on this study, and Mr. Douglas Zhang for his help on language.

Appendix A

Table 7

Values of geometric and surface cover properties for local climate zones (Stewart and Oke, 2012).

Local climate zone (LCZ)	Sky view factor ^a	Aspect ratio ^b	Building surface fraction ^c	Impervious surface fraction ^d	Pervious surface fraction ^e	Height of roughness elements ^f	Terrain roughness class ^g
LCZ 1 Compact high-rise	0.2–0.4	>2	40–60	40–60	<10	>25	8
LCZ 2 Compact midrise	0.3–0.6	0.75–2	40–70	30–50	<20	10–25	6–7
LCZ 3 Compact low-rise	0.2–0.6	0.75–1.5	40–70	20–50	<30	3–10	6
LCZ 4 Open high-rise	0.5–0.7	0.75–1.25	20–40	30–40	30–40	>25	7–8
LCZ 5 Open midrise	0.5–0.8	0.3–0.75	20–40	30–50	20–40	10–25	5–6
LCZ 6 Open low-rise	0.6–0.9	0.3–0.75	20–40	20–50	30–60	3–10	5–6
LCZ 7 Lightweight low-rise	0.2–0.5	1–2	60–90	<20	<30	2–4	4–5
LCZ 8 Large low-rise	>0.7	0.1–0.3	30–50	40–50	<20	3–10	5
LCZ 9 Sparsely built	>0.8	0.1–0.25	10–20	<20	60–80	3–10	5–6
LCZ 10 Heavy industry	0.6–0.9	0.2–0.5	20–30	20–40	40–50	5–15	5–6
LCZ A Dense trees	<0.4	>1	<10	<10	>90	3–30	8
LCZB Scattered trees	0.5–0.8	0.25–0.75	<10	<10	>90	3–15	5–6
LCZC Bush, scrub	0.7–0.9	0.25–1.0	<10	<10	>90	<2	4–5
LCZ D Low plants	>0.9	<0.1	<10	<10	>90	<1	3–4
LCZ E Bare rock or paved	>0.9	<0.1	<10	>90	<10	<0.25	1–2
LCZ F Bare soil or sand	>0.9	<0.1	<10	<10	>90	<0.25	1–2
LCZG Water	>0.9	<0.1	<10	<10	>90	–	1

^a Ratio of the amount of sky hemisphere visible from ground level to that of an unobstructed hemisphere.

^b Mean height-to-width ratio of street canyons (LCZs 1–7), building spacing (LCZs 8–10), and tree spacing (LCZs A–G).

^c Ratio of building plan area to total plan area (%).

^d Ratio of impervious plan area (paved, rock) to total plan area (%).

^e Ratio of pervious plan area (bare soil, vegetation, water) to total plan area (%).

^f Geometric average of building heights (LCZs 1–10) and tree/plant heights (LCZs A–F) (m).

^g Davenport et al. (2000)'s classification of effective terrain roughness (z_0) for city and country landscapes.

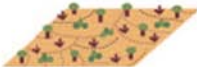
Built types	Definition	Land cover types	Definition
 <p>1. Compact high-rise</p>	Dense mix of tall buildings to tens of stories. Few or no trees. Land cover mostly paved. Concrete, steel, stone, and glass construction materials.	 <p>A. Dense trees</p>	Heavily wooded landscape of deciduous and/or evergreen trees. Land cover mostly pervious (low plants). Zone function is natural forest, tree cultivation, or urban park.
 <p>2. Compact midrise</p>	Dense mix of midrise buildings (3–9 stories). Few or no trees. Land cover mostly paved. Stone, brick, tile, and concrete construction materials.	 <p>B. Scattered trees</p>	Lightly wooded landscape of deciduous and/or evergreen trees. Land cover mostly pervious (low plants). Zone function is natural forest, tree cultivation, or urban park.
 <p>3. Compact low-rise</p>	Dense mix of low-rise buildings (1–3 stories). Few or no trees. Land cover mostly paved. Stone, brick, tile, and concrete construction materials.	 <p>C. Bush, scrub</p>	Open arrangement of bushes, shrubs, and short, woody trees. Land cover mostly pervious (bare soil or sand). Zone function is natural scrubland or agriculture.
 <p>4. Open high-rise</p>	Open arrangement of tall buildings to tens of stories. Abundance of pervious land cover (low plants, scattered trees). Concrete, steel, stone, and glass construction materials.	 <p>D. Low plants</p>	Featureless landscape of grass or herbaceous plants/crops. Few or no trees. Zone function is natural grassland, agriculture, or urban park.
 <p>5. Open midrise</p>	Open arrangement of midrise buildings (3–9 stories). Abundance of pervious land cover (low plants, scattered trees). Concrete, steel, stone, and glass construction materials.	 <p>E. Bare rock or paved</p>	Featureless landscape of rock or paved cover. Few or no trees or plants. Zone function is natural desert (rock) or urban transportation.
 <p>6. Open low-rise</p>	Open arrangement of low-rise buildings (1–3 stories). Abundance of pervious land cover (low plants, scattered trees). Wood, brick, stone, tile, and concrete construction materials.	 <p>F. Bare soil or sand</p>	Featureless landscape of soil or sand cover. Few or no trees or plants. Zone function is natural desert or agriculture.
 <p>7. Lightweight low-rise</p>	Dense mix of single-story buildings. Few or no trees. Land cover mostly hard-packed. Lightweight construction materials (e.g., wood, thatch, corrugated metal).	 <p>G. Water</p>	Large, open water bodies such as seas and lakes, or small bodies such as rivers, reservoirs, and lagoons.
 <p>8. Large low-rise</p>	Open arrangement of large low-rise buildings (1–3 stories). Few or no trees. Land cover mostly paved. Steel, concrete, metal, and stone construction materials.	VARIABLE LAND COVER PROPERTIES	
 <p>9. Sparsely built</p>	Sparse arrangement of small or medium-sized buildings in a natural setting. Abundance of pervious land cover (low plants, scattered trees).	Variable or ephemeral land cover properties that change significantly with synoptic weather patterns, agricultural practices, and/or seasonal cycles.	
 <p>10. Heavy industry</p>	Low-rise and midrise industrial structures (towers, tanks, stacks). Few or no trees. Land cover mostly paved or hard-packed. Metal, steel, and concrete construction materials.	<p>b. bare trees</p>	Leafless deciduous trees (e.g., winter). Increased sky view factor. Reduced albedo.
		<p>s. snow cover</p>	Snow cover >10 cm in depth. Low admittance. High albedo.
		<p>d. dry ground</p>	Parched soil. Low admittance. Large Bowen ratio. Increased albedo.
		<p>w. wet ground</p>	Waterlogged soil. High admittance. Small Bowen ratio. Reduced albedo.

Fig. 12. Definitions of LCZ classes (Stewart and Oke, 2012).

LCZ COMPACT HIGHRISE 1

DEFINITION

Form: Dense mix of tall buildings to tens of stories. Buildings free-standing, closely spaced. Sky view from street level significantly reduced. Buildings of steel, concrete, and glass construction. Land cover mostly paved; few or no trees. High space heating/cooling demand. Heavy traffic flow. **Function:** Commercial (office buildings, hotels); residential (apartment towers). **Location:** Core (downtown, central business district); periphery (highrise subcentre, highrise sprawl). **Correspondence:** UCZ1 (Oke 2004); Dc1 and Dc8 (Ellefsen 1990/91).

ILLUSTRATION

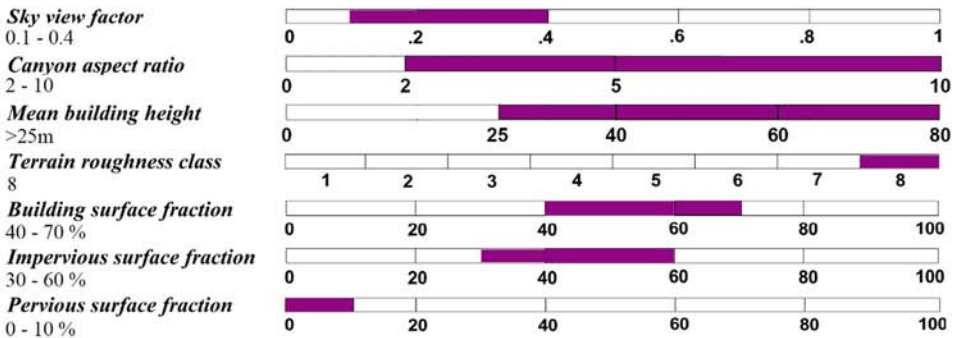
High angle



Low level



Properties in Hong Kong



Properties in Other Cities (Stewart, 2011)

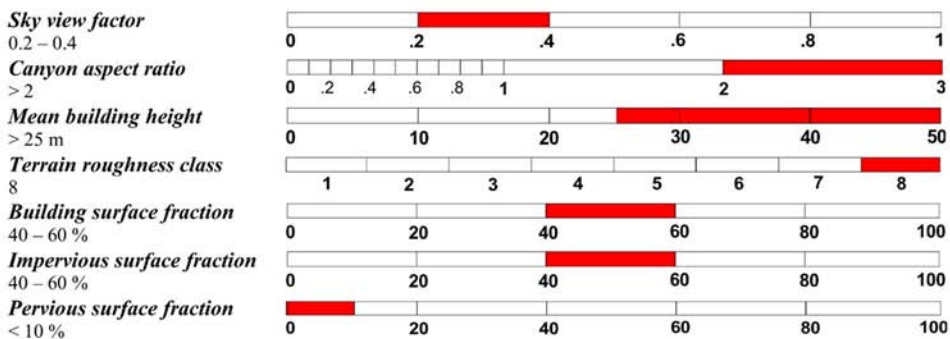


Fig. 13. Datasheet for Local Climate Zone 1.

LCZ COMPACT MIDRISE 2

DEFINITION

Form: Attached or closely spaced buildings 3–9 stories tall. Buildings separated by narrow streets and inner courtyards. Buildings uniform in height. Sky view from street level significantly reduced. Heavy building materials (stone, concrete, brick, tile) and thick roofs and walls. Land cover mostly paved; few or no trees. Moderate space heating/cooling demand. Moderate to heavy traffic flow. **Function:** Residential (multi-unit housing; multistorey tenements); commercial (office buildings, hotels, retail shops); industrial (warehouses, factories). **Location:** Core (old city, old town; inner city, central business district); periphery (high-density sprawl). **Correspondence:** UCZ2 (Oke, 2004); A1, A2, A4, Dc2 (Ellefsen, 1990/91).

ILLUSTRATION

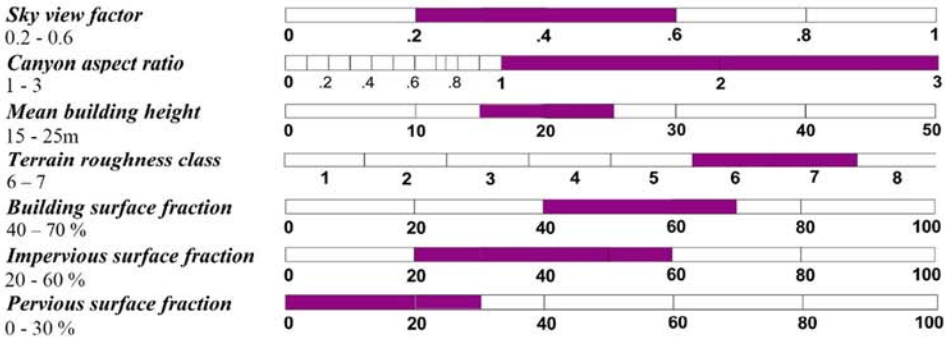
High angle



Low level



Properties in Hong Kong



Properties in Other Cities (Stewart, 2011)

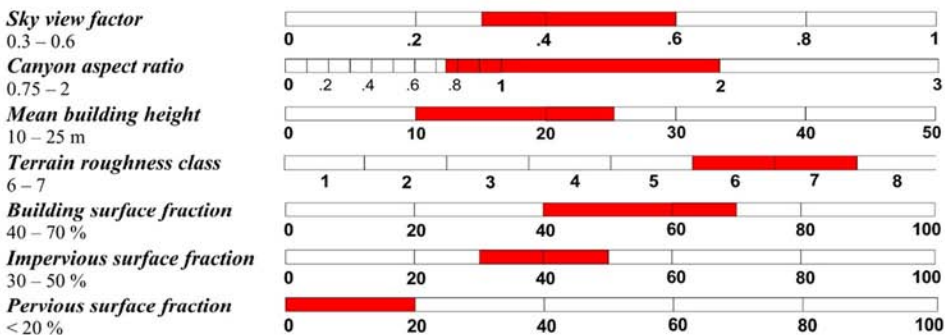


Fig. 14. Datasheet for Local Climate Zone 2.

LCZ COMPACT LOWRISE 3

DEFINITION

Form: Attached or closely spaced buildings 1–3 stories tall. Buildings small and tightly packed along narrow streets, often without discernable alignment. Sky view from street level significantly reduced. Heavy building materials (stone, concrete, brick, tile) and thick roofs and walls. Land cover mostly paved; few or no trees. Moderate space heating/cooling demand. Low-moderate traffic flow. **Function:** Residential (single-unit housing, high-density terrace/row housing); commercial (small retail shops). **Location:** Old or densely populated cities, towns, villages. Core (central or inner city); periphery (high-density sprawl). **Correspondence:** UCZ3 (Oke, 2004); Dc3 (Ellefsen, 1990/91).

ILLUSTRATION

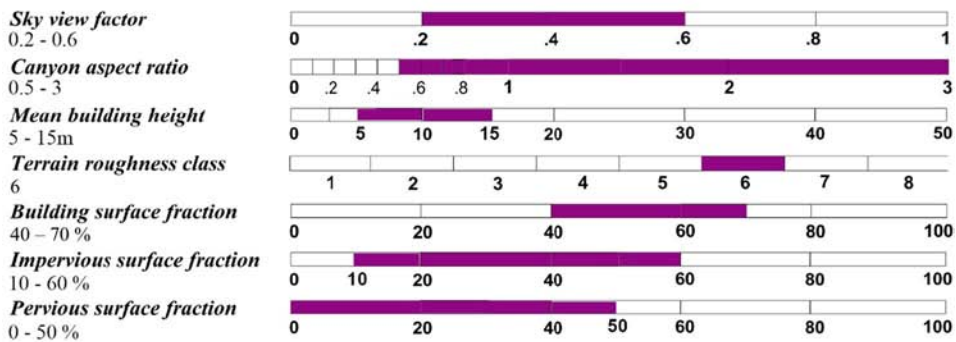
High angle



Low level



Properties in Hong Kong



Properties in Other Cities (Stewart, 2011)

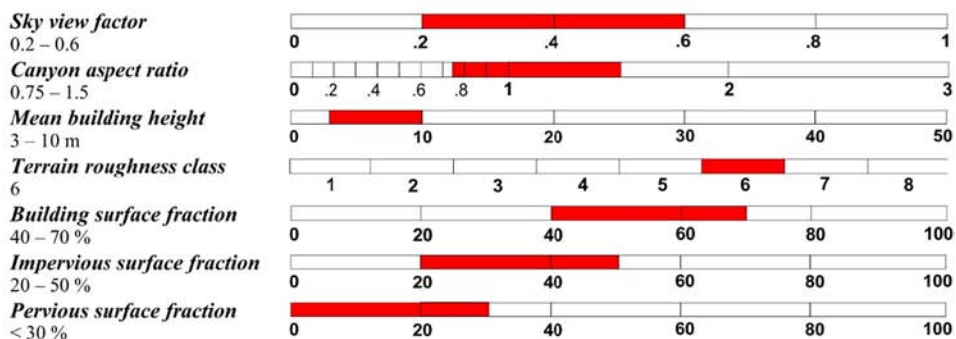


Fig. 15. Datasheet for Local Climate Zone 3.

LCZ OPEN HIGHRISE 4

DEFINITION

Form: Buildings tens of stories tall, set in open, geometric arrangement. Buildings uniform in height, width, and spacing. Sky view from ground level significantly reduced. Heavy building materials (concrete, steel, stone, glass) and thick roofs and walls. Roofs typically flat. Scattered trees and abundant plant cover. Moderate-low space heating/cooling demand. Moderate traffic flow. **Function:** Residential (apartment blocks, highrise housing estates, multistorey tenements). **Location:** Periphery. Densely populated cities. Socialist-style cities. **Correspondence:** Do2 (Ellefsen, 1990/91).

ILLUSTRATION

High angle



Low level



Properties in Hong Kong

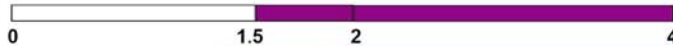
Sky view factor

0.4 - 0.7



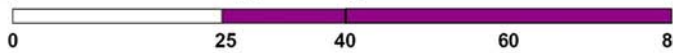
Canyon aspect ratio

1.5 - 4



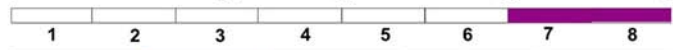
Mean building height

>25m



Terrain roughness class

7 - 8



Building surface fraction

20 - 40 %



Impervious surface fraction

20 - 60 %



Pervious surface fraction

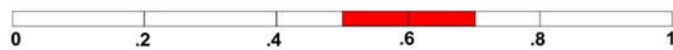
10 - 70 %



Properties in Other Cities (Stewart, 2011)

Sky view factor

0.5 - 0.7



Canyon aspect ratio

0.75 - 1.25



Mean building height

> 25 m



Terrain roughness class

7 - 8



Building surface fraction

20 - 40 %



Impervious surface fraction

30 - 40 %



Pervious surface fraction

30 - 40 %



Fig. 16. Datasheet for Local Climate Zone 4.

LCZ OPEN MIDRISE 5

DEFINITION

Form: Open arrangement of buildings 3–9 stories tall. Sky view from street level slightly reduced. Heavy building materials (concrete, steel, stone, glass) and thick roofs and walls. Scattered trees and abundant plant cover. Low space heating/cooling demand. Low traffic flow. **Function:** Residential (multi-unit housing, multistorey tenements, apartment blocks); institutional (research/business parks, campuses); commercial (office buildings, hotels). **Location:** Periphery. **Correspondence:** UCZ6 (Oke, 2004); Do6 (Ellefsen, 1990/91).

ILLUSTRATION

High angle



Low level



Properties in Hong Kong

Sky view factor

0.4 - 0.8



Canyon aspect ratio

0.5 - 2



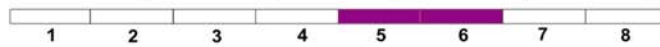
Mean building height

15-25m



Terrain roughness class

5 - 6



Building surface fraction

20 - 40 %



Impervious surface fraction

10 - 60 %



Pervious surface fraction

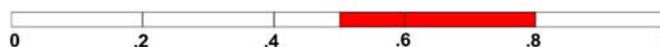
10 - 70 %



Properties in Other Cities (Stewart, 2011)

Sky view factor

0.5 - 0.8



Canyon aspect ratio

0.3 - 0.75



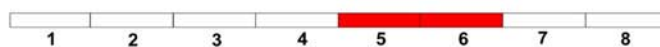
Mean building height

10 - 25 m



Terrain roughness class

5 - 6



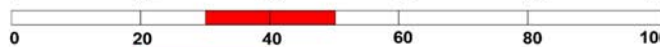
Building surface fraction

20 - 40 %



Impervious surface fraction

30 - 50 %



Pervious surface fraction

20 - 40 %



Fig. 17. Datasheet for Local Climate Zone 5.

LCZ OPEN LOWRISE 6

DEFINITION

Form: Small buildings 1–3 stories tall; detached or attached in rows, often in grid pattern. Sky view from street level slightly reduced. Building materials vary (wood, brick, stone, tile). Scattered trees and abundant plant cover. Low space heating/cooling demand. Low traffic flow. **Function:** Residential (single or multi-unit housing, low density terrace/row housing); commercial (small retail shops). **Location:** City (medium density); periphery (suburbs). Commuter towns. Rural towns. **Correspondence:** UCZ5 (Oke 2004); Do3 (Ellefsen 1990/91).

ILLUSTRATION

High angle



Low level



Properties in Hong Kong

Sky view factor

0.6 - 0.9



Canyon aspect ratio

0.2 - 2



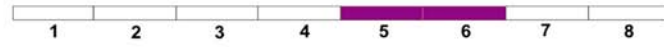
Mean building height

5-15m



Terrain roughness class

5 - 6



Building surface fraction

20 - 40 %



Impervious surface fraction

10 - 60 %



Pervious surface fraction

10 - 70 %



Properties in Other Cities (Stewart, 2011)

Sky view factor

0.6 - 0.9



Canyon aspect ratio

0.3 - 0.75



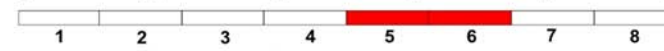
Mean building height

3 - 10 m



Terrain roughness class

5 - 6



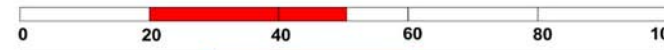
Building surface fraction

20 - 40 %



Impervious surface fraction

20 - 50 %



Pervious surface fraction

30 - 60 %



Fig. 18. Datasheet for Local Climate Zone 6.

References

- Acero, J.A., Arrizabalaga, J., Kupski, S., Katschner, L., 2013. Urban heat island in a coastal urban area in northern Spain. *Theor. Appl. Climatol.* 113 (1–2), 137–154.
- Ali-Toudert, F., Mayer, H., 2006. Numerical study on the effects of aspect ratio and orientation of an urban street canyon on outdoor thermal comfort in hot and dry climate. *Build. Environ.* 41 (2), 94–08.
- ArcGIS, 2011a. How Kriging Works. (from). <http://help.arcgis.com/EN/ARCGISDESKTOP/10.0/HELP/index.html#//009z0000076000000.htm>.
- ArcGIS, 2011b. Understanding a Semivariogram: The Range, Sill, and Nugget. (from). <http://pro.arcgis.com/en/pro-app/help/analysis/geostatistical-analyst/understanding-a-semivariogram-the-range-sill-and-nugget.htm>.
- Bechtel, B., Daneke, C., 2012. Classification of local climate zones based on multiple earth observation data. *IEEE J. Sel. Top. Appl. Earth Obs. Remote Sens.* 5 (4), 1191–1202.
- Bechtel, B., Alexander, P.J., Böhner, J., Ching, J., Conrad, O., Feddema, J., Mills, G., See, L., Stewart, I., 2015. Mapping local climate zones for a worldwide database of the form and function of cities. *ISPRS Int. J. Geo-Inf.* 4:199–219. <http://dx.doi.org/10.3390/ijgi4010199>.
- Brousse, O., Martilli, A., Foley, M., Mills, G., Bechtel, B., 2016. WUDAPT, an efficient land use producing data tool for mesoscale models? Integration of urban LCZ in WRF over Madrid. *Urban Clim.* 17, 116–134.
- Chang, C.H., Goh, K.C., 1999. The Relationship Between Height to Width Ratios and the Heat Island Intensity at 22:00 h for Singapore.
- Chen, L., Ng, E., An, X., Ren, C., Lee, M., Wang, U., He, Z., 2010. Sky view factor analysis of street canyons and its implications for daytime intra-urban air temperature differentials in high-rise, high-density urban areas of Hong Kong: a GIS-based simulation approach. *Int. J. Climatol.* 32 (1), 121–136.
- Cheung, C., Fuller, R., Luther, M., 2005. Energy-efficient envelope design for high-rise apartments. *Energ. Buildings* 37 (1), 37–48.
- Chow, W.T., Pope, R.L., Martin, C.A., Brazel, A.J., 2011. Observing and modeling the nocturnal park cool island of an arid city: horizontal and vertical impacts. *Theor. Appl. Climatol.* 103 (1–2), 197–211.
- Conrad, O., Bechtel, B., Bock, M., Dietrich, H., Fischer, E., Gerlitz, L., Wehberg, J., Wichmann, V., Böhner, J., 2015. System for automated geoscientific analyses (SAGA) v. 2.1. 4. *Geosci. Model Dev.* 8 (7), 1991–2007.
- Couclelis, H., 1992. People manipulate objects (but cultivate fields): beyond the raster-vector debate in GIS. *Theories and Methods of Spatio-temporal Reasoning in Geographic Space*. Springer, pp. 65–77.
- Davenport, A.G., Grimmond, C.S.B., Oke, T.R., Wieringa, J., 2000. Estimating the Roughness of Cities and Sheltered Country. Paper Presented at the 15th Conference on Probability and Statistics in the Atmospheric Sciences/12th Conference on Applied Climatology. American Meteorological Society, Asheville, NC.
- Ellefsen, R., 1991. Mapping and measuring buildings in the canopy boundary layer in ten US cities. *Energ. Buildings* 16 (3), 1025–1049.
- Emmanuel, R., Krüger, E., 2012. Urban heat island and its impact on climate change resilience in a shrinking city: the case of Glasgow, UK. *Build. Environ.* 53, 137–149.
- Gál, T., Bechtel, B., Unger, J., 2015. Comparison of Two Different Local Climate Zone Mapping Methods.
- Hart, M.A., Sailor, D.J., 2009. Quantifying the influence of land-use and surface characteristics on spatial variability in the urban heat island. *Theor. Appl. Climatol.* 95 (3–4), 397–406.
- HKBuildingDepartment, 2009. Sustainable Building Design Guidelines: Practice Note for Authorized Persons, Registered Structural Engineers and Registered Geotechnical Engineers.
- HKGovernment, 2015. Hong Kong: The Facts - Population.
- HKPlanningDepartment, 2014. Land Utilization in Hong Kong. 2014 (Retrieved from). http://www.pland.gov.hk/pland_en/info_serv/statistic/landu.html.
- HKPlanningDepartment, 2016a. Kai Tak Planning Review.
- HKPlanningDepartment, 2016b. Statutory Plan Index. (Retrieved from). http://www.pland.gov.hk/pland_en/info_serv/tp_plan/images/sta_plan.pdf.
- Houet, T., Pigeon, G., 2011. Mapping urban climate zones and quantifying climate behaviors—an application on Toulouse urban area (France). *Environ. Pollut.* 159 (8), 2180–2192.
- Knutson, T.R., Tuleya, R.E., Kurihara, Y., 1998. Simulated increase of hurricane intensities in a CO₂-warmed climate. *Science* 279 (5353), 1018–1021.
- Lau, K., Ren, C., Shi, Y., Zheng, V., Yim, S., Lai, D., 2015. Determining the optimal size of local climate zones for spatial mapping in high-density cities. Paper Presented at the 9th International Conference on Urban Climate. France, Toulouse.
- Lecante, F., Bouyer, J., Claverie, R., Pétrissans, M., 2015. Using local climate zone scheme for UHI assessment: evaluation of the method using mobile measurements. *Build. Environ.* 83, 39–49.
- Lelovics, E., Unger, J., Gál, T., 2014. Design of an urban monitoring network based on local climate zone mapping and temperature pattern modelling. *Clim. Res.* 60, 51–62.
- Liu, L., Zhang, Y., 2011. Urban heat island analysis using the Landsat TM data and ASTER data: a case study in Hong Kong. *Remote Sens.* 3 (7), 1535–1552.
- Memon, R.A., Leung, D.Y., Liu, C.-H., 2010. Effects of building aspect ratio and wind speed on air temperatures in urban-like street canyons. *Build. Environ.* 45 (1), 176–188.
- Middel, A., Häb, K., Brazel, A.J., Martin, C.A., Guhathakurta, S., 2014. Impact of urban form and design on mid-afternoon microclimate in phoenix local climate zones. *Landsc. Urban Plan.* 122, 16–28.
- Mills, G., Ching, J., See, L., Betschel, B., 2015. An Introduction to the WUDAPT Project. Paper Presented at the 9th International Conference on Urban Climate.
- Ng, E., 2012. Towards planning and practical understanding of the need for meteorological and climatic information in the design of high-density cities: a case-based study of Hong Kong. *Int. J. Climatol.* 32 (4), 582–598.
- Ng, E., Ren, C., 2015. *The Urban Climatic Map: A Methodology for Sustainable Urban Planning*. Routledge.
- Ng, E., Yuan, C., Chen, L., Ren, C., Fung, J.C., 2011. Improving the wind environment in high-density cities by understanding urban morphology and surface roughness: a study in Hong Kong. *Landsc. Urban Plan.* 101 (1), 59–74.
- Ng, E., Yau, R., Wong, K.S., Ren, C., 2012. Final Report of Hong Kong Urban Climatic Map and Standards for Wind Environment - Feasibility Study.
- Oke, T.R., 1981. Canyon geometry and the nocturnal urban heat island: comparison of scale model and field observations. *J. Climatol.* 1 (3), 237–254.

- Oke, T.R., 2004. Initial Guidance to Obtain Representative Meteorological Observations at Urban Sites.
- Orlowsky, B., Gerstengarbe, F.-W., Werner, P., 2008. A resampling scheme for regional climate simulations and its performance compared to a dynamical RCM. *Theor. Appl. Climatol.* 92 (3–4), 209–223.
- Perera, N.G.R., Emmanuel, R., Mahanama, P.K.S., 2012. Mapping “Local Climate Zones” and Relative Warming Effects in Colombo, Sri Lanka. Paper Presented at the 8th International Conference on Urban Climate, Dublin, Ireland.
- Ren, C., 2010. Application of Urban Climatic Map to Urban Planning of High Density Cities - A Case Study of Hong Kong (Doctoral). The Chinese University of Hong Kong.
- Ren, C., Ng, E.Y.y., Katzschner, L., 2011. Urban climatic map studies: a review. *Int. J. Climatol.* 31 (15), 2213–2233.
- Ren, C., Lau, K.L., Yiu, K.P., Ng, E., 2013. The application of urban climatic mapping to the urban planning of high-density cities: the case of Kaohsiung, Taiwan. *Cities* 31, 1–16.
- Ren, C., Cai, M., Wang, R., Xu, Y., Ng, E., 2016. Local Climate Zone (LCZ) Classification by Using the Method of World Urban World Urban Database and Access Portal Tools (WUDAPT): A Case Study in Wuhan and Hangzhou. Paper Presented at the Fourth International Conference on Countermeasure to Urban Heat Island Singapore.
- Ren, C., Fung, J.C.-H., Tse, J.W.P., Wang, R., Wong, M.M.F., Xu, Y., 2017. Implementing WUDAPT product into urban development impact analysis by using WRF simulation result—a case study of the Pearl River Delta Region. Paper Presented at The 13th Symposium on Urban Environment.
- Santamouris, M., Papanikolaou, N., Koronakis, I., Livada, I., Asimakopoulos, D., 1999. Thermal and air flow characteristics in a deep pedestrian canyon under hot weather conditions. *Atmos. Environ.* 33 (27), 4503–4521.
- Spronken-Smith, R.A., Oke, T.R., 1998. The thermal regime of urban parks in two cities with different summer climates. *Int. J. Remote Sens.* 19 (11), 2085–2104.
- Stewart, I.D., 2011. Redefining the Urban Heat Island. University of British Columbia (Retrieved from). <https://circle.ubc.ca/handle/2429/38069>.
- Stewart, I.D., Oke, T.R., 2012. Local climate zones for urban temperature studies. *Bull. Am. Meteorol. Soc.* 93 (12), 1879–1900.
- Stewart, I.D., Oke, T.R., Krayenhoff, E.S., 2014. Evaluation of the ‘local climate zone’ scheme using temperature observations and model simulations. *Int. J. Climatol.* 34 (4), 1062–1080.
- Svensson, M.K., 2004. Sky view factor analysis—implications for urban air temperature differences. *Meteorol. Appl.* 11 (03), 201–211.
- Unger, J., 2004. Intra-urban relationship between surface geometry and urban heat island: review and new approach. *Clim. Res.* 27, 253–264.
- Unger, J., Lelovics, E., Gál, T., 2014. Local Climate Zone mapping using GIS methods in Szeged. *Hung. Geogr. Bull.* 63 (1), 29–41.
- Upmanis, H., Chen, D., 1999. Influence of geographical factors and meteorological variables on nocturnal urban-park temperature differences—a case study of summer 1995 in Göteborg, Sweden. *Clim. Res.* 13 (2), 125–139.
- Weier, J., Herring, D., 2000. Measuring Vegetation (NDVI & EVI). (from). <http://earthobservatory.nasa.gov/Features/MeasuringVegetation/>.
- Wong, N.H., Yu, C., 2005. Study of green areas and urban heat island in a tropical city. *Habitat Int.* 29 (3), 547–558.
- Xu, S., 2009. An approach to analyzing the intensity of the daytime surface urban heat island effect at a local scale. *Environ. Monit. Assess.* 151 (1–4), 289–300.
- Zheng, Y., 2016. Planning Strategies for Urban Heat Island Mitigation: An Application of Local Climate Zone into the High-density City of Hong Kong. (Doctor). The Chinese University of Hong Kong.
- Zheng, Y., Ren, C., Shi, Y., Lau, K.L., Yim, H.L.S., Lai, D., Ho, J., NG, E., 2015. Applying “Local Climate Zone (LCZ)” into a High-density High-rise Cities - A Pilot Study in Hong Kong. Paper Presented at the 9th International Conference on Urban Climate, Toulouse, France.